

Application of High-Frequency Dielectric Logging Technology for Shale Oil Production

Chen Li^{1, 2}, Shaogui Deng^{1, *}, Zhiqiang Li²,
Yiren Fan¹, Jingjing Zhang², and Jutao Yang²

Abstract—Shale oil and gas are unconventional oil and gas resources that can be used as alternative energy sources in the future. Shale reservoirs are the new growth point for the exploitation of oil and gas and development of China’s oil and gas industry. The heterogeneity of the shale stratum determines the complexity of its mining. Accurate identification and detection of its oil-bearing characteristics are principal tasks in the oil shale deposit evaluation and economically exploitable interval division. Dielectric logging cannot rely on traditional resistivity logging curves, and it is not affected by the formation water salinity, which can provide the formation water porosity. Combined with other types of logging, it can effectively evaluate the formation oil saturation. In this study, we applied a new type of high-frequency dielectric logging tool in the production of shale oil, developed by the 22nd Institute of China Electronics Technology Group Corporation, based on different dielectric constants of oil, rock matrix, and water. We first introduced the principle of dielectric logging and the major advantages of the dielectric logging tool, and further proposed a new complex refractive index model with clay correction and explained the processing methods, which improved the accuracy of calculating the formation water saturation. Furthermore, the developed technology was applied and evaluated in the Songliao Basin.

1. INTRODUCTION

Shale oil is an essential alternative unconventional oil resource stored mainly in shale reservoirs with low porosity and permeability. The “oil and gas” statistics of the United States show that there are approximately 11–13 trillion tons of shale oil reserves worldwide, which is significantly greater than conventional oil reserves. Currently, shale oil has led to the rapid development of the oil industry in North America [1]. The Ordos Basin, Sichuan Basin, and Songliao Basin in China hold abundant amounts of shale oil and gas, thus providing good prospects for exploration and exploitation [2–4]. Furthermore, the development of shale oil varies in China and other countries based on the key technologies used for exploration and production. Therefore, finding an effective technology for the investigation and development of shale oil based on the characteristics of formation conditions and the enrichment mechanism of continental shale resources in China is an urgent problem that needs to be solved.

In recent years, many scholars and institutions have analyzed the logging evaluation of shale oil and gas bearing shale to explore new technologies and applications suitable for shale oil exploration. Heidari and Torres-Verdin studied a method of comprehensive evaluation of oil shale using density, neutron, PE, natural gamma ray spectroscopy, and resistivity logging data by classifying the composition of oil shale into skeleton minerals, clay, organic matter, and pores (hydrocarbons, movable water, and

Received 14 August 2021, Accepted 13 September 2021, Scheduled 24 September 2021

* Corresponding author: Shaogui Deng (Dengshaogui2021@126.com).

¹ School of Geosciences, China University of Petroleum (East China), Changjiangxi Road 66, Qingdao 266580, China. ² China Research Institute of Radiowave Propagation, Jianshedong Road 84, Xinxiang 453000, China.

bound water) [5]. In 2010, a company called AMSO calculated the content of kerogen used for drilling shale in the Green River Basin using a density instrument and nuclear magnetic resonance porosity [6]. In 2007, Gale et al. studied the natural fractures of oil shale in the Barnett Basin and the importance of fractures in hydraulic fracturing [7].

The geological structure of shale reservoir is complex. For example, the distribution of faults may lead to formation water entering the shale reservoir and reducing the permeability and oil or gas saturation. The identification and evaluation of oil saturation by resistivity logging are complex. Based on the dielectric correlation between formation water and other formation components (minerals and stored fluids), the combination of dielectric logging and other types of logging can yield the water porosity and water mineralization of the formation; this helps in evaluating the oil saturation of the formation, which can provide useful insights and references for shale oil and gas exploitation.

2. PRINCIPLES OF THE DIELECTRIC LOGGING TECHNOLOGY

According to the principle of the dielectric logging technology, high-frequency electromagnetic waves are radiated to the formation around a well, transmitted through the formation, and measured at the receiving antenna; these waves are a function of the working frequency, dielectric constant of formation, conductivity of formation, and distance between the transmitting and receiving antennas. Several interactions occur between high-frequency electromagnetic waves and the fluids and minerals in the formation during propagation, resulting in changes in the amplitude and phase of the electromagnetic waves. The amplitude and phase of the signal, acquired using a high-frequency circuit system, are processed and inverted to obtain the dielectric constant of the formation [8–10].

Because water, rock matrix, oil, and gas have different dielectric constants (as summarized in Table 1), they can be used to identify and distinguish between the oil and water layers. Simultaneously, because the dielectric logging tool is sensitive to water in the formation pores, it is used to calculate the water-bearing porosity based on the measured dielectric constant value independent of resistivity; thus, the problem related to conventional interpretation that must know the formation water resistivity and depends on the interpretation of resistivity curve can be avoided [9–11]. Moreover, it can effectively evaluate and identify unconventional oil and gas resources, such as reservoirs comprising fresh water or unknown salinity water, heavy oil, and shale oil and gas.

Table 1. Dielectric permittivity of minerals and fluids [12].

Common minerals and fluids	Dielectric constants
Quartz	4.4
Oil	2.0–2.4
Gas	1
Sandstone	4.65
Dolomite	6
Limestone	7.5–9.2
Shale	5–25
Dry colloid	5.76
Water*	58–78

*Based on frequency, pressure, temperature, and salinity.

3. NEW HIGH-FREQUENCY DIELECTRIC LOGGING TOOL

The dielectric logging technology has been applied in the field of petroleum logging since the end of 1970s [12]. Scientific research organizations have developed different dielectric logging tools with different working frequencies. In 1997, Daqing, a branch of the China Petroleum Logging Corporation,

developed a high-frequency radio wave transmission logging tool with a single frequency of 60 MHz [13]. Furthermore, Schlumberger developed a 1.1 GHz dielectric logging tool (EPT), and Baker Hughes developed a 47 and 200 MHz dual-frequency dielectric logging tool [14]. However, owing to the limitations of borehole conditions, general measurement accuracy, and lack of quality control, the dielectric logging tools developed in the past are not widely used.

Therefore, the 22nd Institute of China Electronics Technology Group Corporation developed a new high-frequency dielectric logging tool, a new generation of downhole logging tools with microwave bands and multi-antennas, comprising advanced hydraulic pushback systems and integrated digital dielectric measuring probes that help in overcoming the limitations of the previously discussed dielectric logging tools; this tool can be used for the precise identification and evaluation of complex reservoir fluids, as shown in Figure 1.

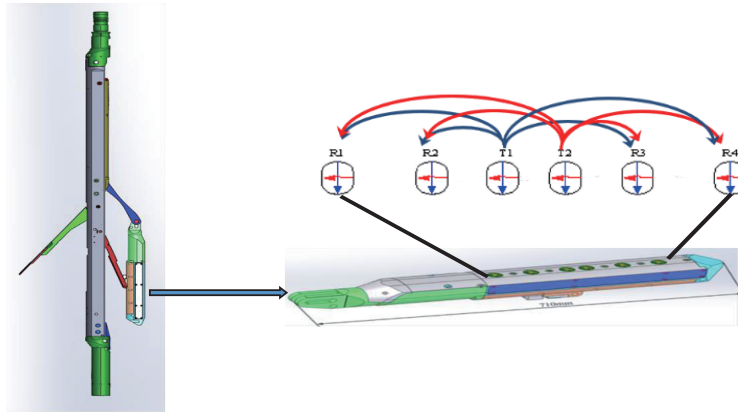


Figure 1. A new high-frequency dielectric logging tool and dual polarization antenna.

The integrated digital design comprises two symmetrical complementary transmitting antennas, T1 and T2, in the middle and four receiving array antennas, R1, R2, R3, and R4, placed on both sides; it achieves 1 GHz electromagnetic wave transmission and the digital process of receiving signals. The spacing between the antennas is 6–6–4–6–6 cm. Additionally, the symmetrical, complementary, and differential measurement modes were adopted to reduce the error influence of the borehole and measurement circuit channel and evaluate the 16 original signal amplitude and phase curves, including VA1, VA2, VA3, and VA4 and VP1, VP2, VP3, and VP4, which are the amplitude and phase information of the original signal in the vertical polarization direction of the receiving antennae R1, R2, R3, and R4, respectively; and HA1, HA2, HA3, and HA4 and HP1, HP2, HP3, and HP4, which are the amplitude and phase information of the original signal in the horizontal polarization direction of the receiving antennae R1, R2, R3, R4, respectively. Lastly, four dielectric constant and resistivity curves were obtained by inversion, including VD41, which is the vertical dielectric constant obtained by inverting the amplitude and phase of the original signal received by receivers 4 and 1; HD32, which is the vertical dielectric constant obtained by inverting the amplitude and phase of the original signal received by receivers 3 and 2; VR41, which is the inversion of the amplitude and phase of the original signal received by receivers 4 and 1 to obtain the vertical formation resistivity; and HR32, which is the inversion of the amplitude and phase of the original signal received by receivers 3 and 2 to obtain the vertical formation resistivity.

The advanced hydraulic pushback system integrates the hydraulic system using a balancing device, uses new hydraulic components such as motors, pumps, and valve groups, and adopts an eccentric design for the upper and lower joints as well as a hinge connection for the upper and lower joints and the main rod, which play the role of flexible nipple and improve the sticking effect of the new dielectric measuring probe, as shown in Figure 2.

The main advantages of the dielectric logging tool are as follows: its working frequency is 1 GHz, which reduces the influence of rock and water salinity formation on the measurement of dielectric parameters. The high vertical resolution of formation (4 cm) can be used to effectively identify the heterogeneous layer and accurately interpret the thin layer; moreover, it helps in the accurate analysis



Figure 2. Physical diagram of SHAD-2000 high-frequency dielectric logging tool.

and interpretation of complex fluids in micro-thin layer, to improve the resolution in formation porosity evaluation. The horizontal and vertical dual-polarization array antenna provides multiple depth logging curves, which can be used to measure the horizontal and vertical permittivity and detect the anisotropy of the formation. The theoretical detection depth is approximately 10–25 cm.

4. APPLICATION OF DIELECTRIC LOGGING TECHNOLOGY IN FLUID EVALUATION OF A COMPLEX RESERVOIR

In the early 1980s, the dielectric propagation time and attenuation were measured using a dielectric logging tool; these parameters were used by logging analysts to evaluate the petrophysical properties of a medium. Although a lossless travel-time method was proposed for calculating the water porosity based on the propagation time of high-frequency electromagnetic waves, the method only considered the formation water and excluded oil, gas, and rock matrix, which resulted in inaccurate calculations of the water-bearing pores. Furthermore, a mixing law was proposed for calculating the formation water porosity [15–19]. The mixing law considers the formation water, oil, and gas in the pore and rock skeleton; however, it adopts a pure rock skeleton with single component without considering the actual formation. The formation skeleton is usually heterogeneous. Generally, the solid part of a reservoir contains a certain amount of argillaceous. Therefore, to accurately evaluate the formation water porosity, in this study, we propose a complex refractive index model (CRIM) with argillaceous correction (as shown in Formula (1)) and integrated the output curve parameters of the dielectric logging tool and those of the conventional logging tool to process the dielectric data and obtained the porosity and salinity of formation water (as shown in Figure 3).

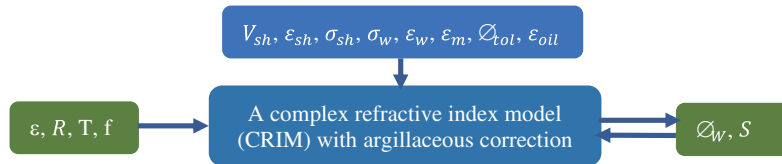


Figure 3. Schematic of data processing in the dielectric interpretation model.

The CRIM with argillaceous correction is given as:

$$\sqrt{\varepsilon + i \frac{1}{2\pi f \varepsilon_0 R}} = \phi_w \sqrt{\varepsilon_w(T, S) + i \frac{\sigma_w(T, S)}{2\pi f \varepsilon_0}} + V_{sh} \sqrt{\varepsilon_{sh} + i \frac{\sigma_{sh}}{2\pi f \varepsilon_0}} + (\phi_{tol} - \phi_w) \sqrt{\varepsilon_{oil}} + (1 - V_{sh} - \phi_{tol}) \sqrt{\varepsilon_m} \quad (1)$$

Here, ε denotes the formation dielectric constant; R is the formation resistivity; $\varepsilon_w(T, S)$ represents the value of the water dielectric constant adjusted to downhole conditions; $\sigma_w(T, S)$ denotes the conductivity value of water adjusted to downhole conditions; f is the working frequency value of the instrument 1e9Hz; ε_0 indicates that the vacuum dielectric constant is 8.852×10^{-12} ; V_{sh} indicates the mud content; ε_{sh} denotes the argillaceous dielectric constant; σ_{sh} is the argillaceous conductivity; ε_m represents the dielectric constant of rock skeleton; ε_{oil} is the dielectric constant of oil; ϕ_w represents water porosity; ϕ_{tol} represents the total porosity; T represents the formation temperature; and S is the salinity of formation water.

Formula (1) is decomposed into real and imaginary parts to obtain the water porosity and formation water dielectric constant.

The real part of Formula (1) is given as:

$$re \left\{ \sqrt{\varepsilon + i \frac{1}{2\pi f \varepsilon_0 R}} \right\} = \phi_w re \left\{ \sqrt{\varepsilon_w(T, S) + i \frac{\sigma_w(T, S)}{2\pi f \varepsilon_0}} \right\} + V_{sh} re \left\{ \sqrt{\varepsilon_{sh} + i \frac{\sigma_{sh}}{2\pi f \varepsilon_0}} \right\} + (\phi_{tol} - \phi_w) \sqrt{\varepsilon_{oil}} + (1 - V_{sh} - \phi_{tol}) \sqrt{\varepsilon_m} \quad (2)$$

After Formula (2) is sorted, Formula (3) can be given as:

$$\phi_w = \frac{re \left\{ \sqrt{\varepsilon + i \frac{1}{2\pi f \varepsilon_0 R}} \right\} - \sqrt{\varepsilon_m} - \phi_{tol} \sqrt{\varepsilon_{oil}} + \phi_{tol} \sqrt{\varepsilon_m}}{re \left\{ \sqrt{\varepsilon_w(T, S) + i \frac{\sigma_w(T, S)}{2\pi f \varepsilon_0}} \right\} - \sqrt{\varepsilon_{oil}}} - V_{sh} \frac{re \left\{ \sqrt{\varepsilon_{sh} + i \frac{\sigma_{sh}}{2\pi f \varepsilon_0}} \right\} - \sqrt{\varepsilon_m}}{re \left\{ \sqrt{\varepsilon_w(T, S) + i \frac{\sigma_w(T, S)}{2\pi f \varepsilon_0}} \right\} - \sqrt{\varepsilon_{oil}}} \quad (3)$$

$$\varepsilon_w(T, S) = re \left\{ \left(\frac{\left(\sqrt{\varepsilon + i \frac{1}{2\pi f \varepsilon_0 R}} - V_{sh} \sqrt{\varepsilon_{sh} + i \frac{\sigma_{sh}}{2\pi f \varepsilon_0}} - (1 - V_{sh} - \phi_{tol}) \sqrt{\varepsilon_m} - (\phi_{tol} - \phi_w) \sqrt{\varepsilon_{oil}} \right)^2}{\phi_w} \right) \right\} \quad (4)$$

In this formula, $re\{\}$: represents the real part; ε , R , T are measured by the dielectric logging tool; V_{sh} , σ_{sh} , and ϕ_{tol} are obtained by conventional logging; $f = 1e9Hz$, $\varepsilon_0 = 8.852 * 1e - 12$, and ε_{oil} can be obtained from Table 1; $\varepsilon_w(T, S)$ and $\sigma_w(T, S)$ can be obtained from the following formulas and data processing flow based on iterative algorithms. ε_m and ε_{sh} are determined by combining the theoretical value and dielectric curve of the standard sandstone and mudstone sections, respectively.

The water complex permittivity is known to vary with the frequency of operation, pressure, temperature, and salinity. We calculated the water bearing porosity for accurate inversion, ϕ_w . The complex permittivity of water must be adjusted to the downhole conditions: $\varepsilon_w^*(T, S)$. Based on the laboratory test data and method [20], the formation water conductivity and dielectric constant formulas were fitted in this study.

$$\sigma_w(T, S) = S^{0.9}(a + bT + c \ln(S) + dT^2 + e(\ln S)^2 + fT \ln(S) + gT^3 + h(\ln S)^3 + iT(\ln(S)^2) + jT^2 \ln(S)) \quad (5)$$

Here, $a = 0.429$, $b = 0.003$, $c = -0.265$, $d = 1.27e - 05$, $e = 0.073$, $f = 0.0008$, $g = -2.87e - 08$, $h = -0.007$, $i = -0.000121$, and $j = -2.311e - 06$.

$$\varepsilon_w(T, S) = 87.2 - 0.374T - 0.223S + 0.0006T^2 + 0.00027S^2 + 0.001TS \quad (6)$$

The salinity of formation water can be deduced from Formula (5).

$$S = \frac{\sqrt{(-0.223 + 0.001T)^2 - 4 \times 0.00027(87.2 - 0.374T + 0.0006T^2 - \varepsilon_w(T, S))} - (-0.223 + 0.001T)}{2 \times 0.00027} \quad (7)$$

The data calculation and processing steps are shown in Figure 4 and explained below.

Step 1: The initial value of S is set to 1, and the relevant parameters, i.e., V_{sh} , ε_{sh} , σ_{sh} , ε_m , ϕ_{tol} , ε_{oil} , ε , R , T , and f , are substituted into Formulas (5) and (6) to calculate $\sigma_w(T, S)$ and $\varepsilon_w(T, S)$.
 Step 2: $\sigma_w(T, S)$ and $\varepsilon_w(T, S)$, obtained in the first step, are substituted into Formula (3) with related parameters to obtain ϕ_w .

Step 3: ϕ_w , obtained in the second step, is substituted into Formula (4) with related parameters to calculate $\varepsilon_w(T, S)$.

Step 4: $\varepsilon_w(T, S)$, obtained in the third step, is substituted into Formula (7) with related parameters to calculate S .

Step 5: S , obtained in the fourth step, is substituted into Formulas (5) and (6); now, this value is given to Step 1 for iterative calculation, and S is updated for each calculation. When the given condition, the number of iterations is equal to 20 or S converges with ϕ_w , is satisfied, only then the values of S and ϕ_w are obtained; otherwise, S gets updated, and calculation continues.

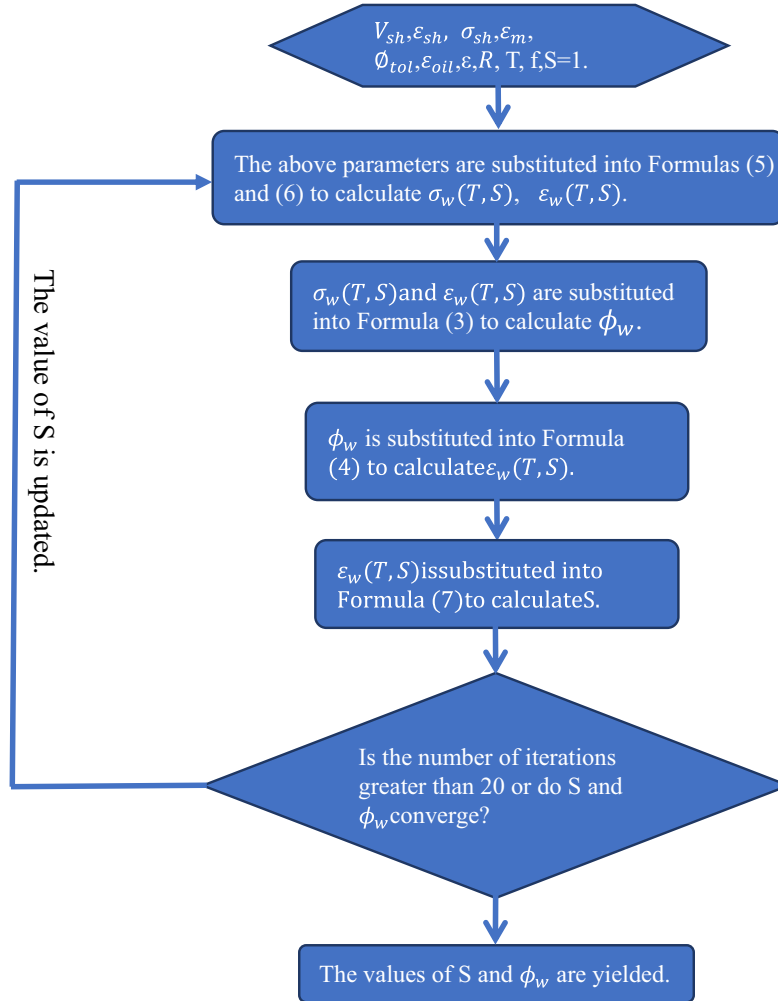


Figure 4. Data processing flowchart.

5. APPLICATIONS OF DIELECTRIC LOGGING IN SHALE RESERVOIR

The Songliao Basin, located in Northeast China, is a large Mesozoic Cenozoic sedimentary superimposed basin that contains rich oil shale resources associated with oil and gas. The oil shale of Qingshankou Formation and Nenjiang Formation constitutes the main oil source rock series in the south of Songliao Basin. The implementation of the new high-frequency dielectric logging technology for tentative exploration in the shale oil layer of the Songliao Basin has important practical and economic benefits. The results of dielectric logging interpretation of a shale oil well in Nenjiang Formation are shown in Figure 5.

The first curve is the well depth curve. The well section with a depth of 2354–2389.1 m is an unconventional shale oil reservoir, whereas the one with a depth of 2389.1–2391.4 m is a conventional sandstone mudstone reservoir. In the second curve, the GR curve is a conventional gamma logging curve and can be used for lithology identification to provide formation shale content. CAL is well diameter curve, which reflects the well wall characteristics, such as diameter reduction and expansion, and BS is the diameter of drilling bit.

In the third channel, the curves RT10 and RT20 and RT30 and RT60 and RT90 are the formation resistivity curves measured by conventional array induction logging tool (10 kHz~150 kHz), and there

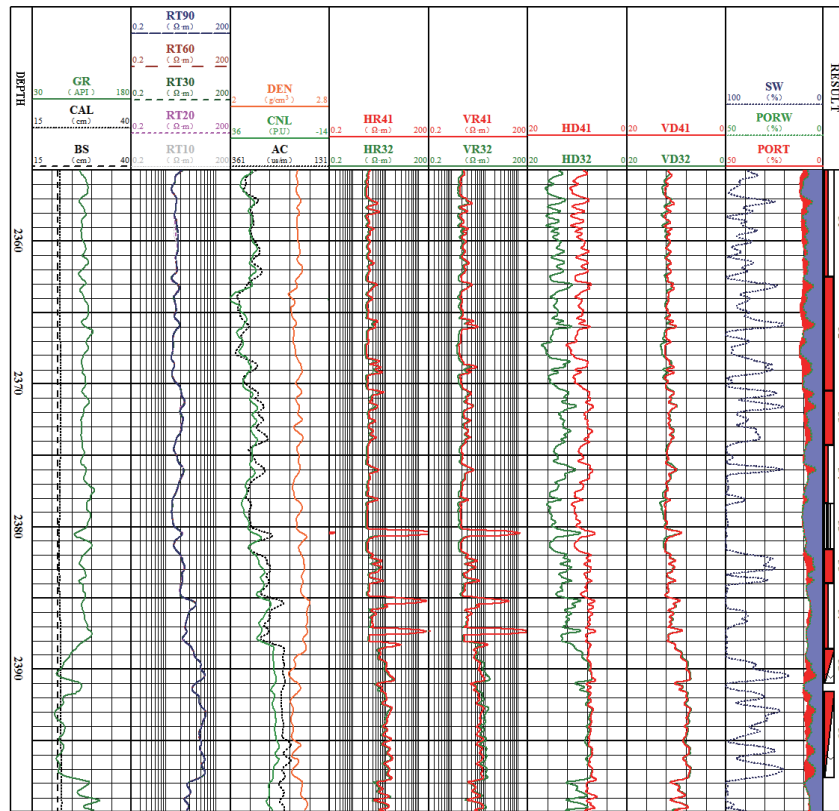


Figure 5. Interpretation results of shale oil high-frequency array dielectric logging in oilfield.

Table 2. Data sheet of shale oil well test production.

Date	Operation mode	Oil production (T)	Water outflow (T)
2020.8.24	Drainage	7.02	28.9
2020.8.23	Drainage	6.3	35.7
2020.8.22	Drainage	5.64	37
2020.8.21	Drainage	4.02	51.8

is little difference in the whole section of resistivity curves. So, it is difficult to directly evaluate the formation storage oil and gas characteristics from the resistivity curves measured by conventional induction logging tool. In the fourth channel, DEN is the compensated density logging curve; CNL is the compensated neutron; and AC is the acoustic logging, which can provide the total porosity of the formation. In the fifth and sixth channels, the curves HR41 and HR32 and VR41 and VR32 are the resistivity curves in the formation horizontal and vertical polarization directions, respectively, as determined using a dielectric instrument. In the seventh and eighth channels, the curves HD41 and HD32 and VD41 and VD32 are the dielectric parameter values in the formation’s horizontal and vertical polarization directions, respectively, as determined using a dielectric logging tool. From the formation dielectric parameter curve provided by the dielectric logging tool, the dielectric constant of oil-rich layers (31, 33, 36, 38, and 39) was slightly lower than that of the less oil-bearing layer (35). In the ninth channel, SW and PORW are the formation water mineralization and porosity calculated based on the complex refractive index (CRIM) model and processing flow proposed in this paper, respectively. PORT is the total formation porosity (red solid line) calculated via neutron density intersection. The blue region

(the intersection of the water bearing porosity curve and right boundary) represents the water-bearing region of the formation, and the red region (the intersection of the total porosity curve and water bearing porosity curve) represents the oil-bearing porosity region of the formation, which can conveniently and directly evaluate the oil-bearing characteristics of the formation and comprehensively calculate the oil saturation of the formation. Through the ratio between the oil-bearing porosity and total porosity curve, the following oil saturation values were obtained for various layers: layer 31 = 18.49%, layers 32 and 33 = 23.98%, layers 34 and 35 = 9.09%, layer 36 = 28.06%, layer 37 = 12.55%, and layers 38 and 39 = 32.27%. Through comprehensive judgment, layers 32, 33, and 36 were determined to be class I oil layers; layers 31, 34, 35, and 37 were determined to be class II oil layers; and layers 38 and 39 were defined as the oil-water layer.

The perforated intervals of this well are on layers 32, 33, 36, 38, and 39. Finally, the well obtained a high-yield oil flow of 7T per day in the Shenhuxiang pure shale reservoir (as shown in Table 2). The oil production data of perforation tests and production effectively verify the evaluation results of dielectric logging; they also confirm that high-frequency dielectric logging can provide useful insights for the exploitation and production of shale oil in oilfields.

6. CONCLUSIONS

In this study, we proposed a CRIM with the shale correction technology to calculate water-bearing pores by measuring the dielectric constant of rocks and fluids through high-frequency electromagnetic waves using a high-frequency dielectric logging tool. Combined with other types of logging, this high-frequency dielectric logging technology can calculate the formation water porosity and mineralization, thus helping in the evaluation of formation oil-bearing characteristics. The new generation of dielectric logging tools were applied to the exploration and identification of shale reservoirs in the Songliao Basin, which provided insightful references for the exploitation of shale oil in oilfields. Because the proposed model is only limited to application in the Songliao Basin, the selection and setting of the model parameters are limited. However, the proposed model has a certain reference significance to provide a convenient and efficient shale reservoir mining method for mining other shale reservoirs in China.

ACKNOWLEDGMENT

This work was supported by the National Natural Science Foundation of China (Grant No. 42074134) and the Major Science and Technology Project of CNPC (Grant No. ZD2019184001).

REFERENCES

1. Thomas, M., N. Pidgeon, and M. Bradshaw, "Shale development in the US and Canada: A review of engagement practice," *The Extractive Industries and Society*, Vol. 5, No. 4, 557–569, 2018.
2. Hu, S., W. Zhao, L. Hou, Z. Yang, R. Zhu, S. Wu, B. Bai, and J. Xu, "Development potential and technical strategy of continental shale oil in China," *Petroleum Exploration and Development*, Vol. 47, No. 4, 877–887, 2020.
3. Zhang, P., D. Misch, H. Fei, N. Kostoglou, R. F. Sachsenhofer, L. Zhaojun, M. Qingtao, and A. Bechtel, "Porosity evolution in organic matter-rich shales (Qingshankou Fm.; Songliao Basin, NE China): Implications for shale oil retention," *Marine and Petroleum Geology*, Vol. 130, 105139, 2021.
4. Liu, B., J. Sun, Y. Zhang, J. He, X. Fu, L. Yang, J. Xing, and X. Zhao, "Reservoir space and enrichment model of shale oil in the first member of Cretaceous Qingshankou Formation in the Changling Sag, southern Songliao Basin, NE China," *Petroleum Exploration and Development*, Vol. 48, No. 3, 608–624, 2021.
5. Heidari, Z. and C. Torres-Verdin, "Quantitative method for estimating total organic carbon and porosity and for diagnosing mineral constituents from well logs in shale-gas formations," *SPWLA 52nd Annual Logging Symposium, Colorado Springs, Colorado*, 2011.

6. Grau, J., M. Herron, and S. Herron, *Organic Carbon Content of the Green River Oil Shale from Nuclear Spectroscopy Logs*, Colorado School of Mines, Golden, Colorado, 2010.
7. Gale, J. F. W., R. M. Reed, and J. Holder, "Natural fractures in the Barnett shale and their importance for hydraulic fracture treatments," *AAPG Bulletin*, Vol. 91, No. 4, 603–622, 2007.
8. Lewis, R., D. Ingraham, and M. Pearcy, "New evaluation techniques for gas shale reservoirs," *Reservoir Symposium*, Schlumberger, 2004.
9. Dunn, J. M., "Lateral wave propagation in a three-layered medium," *Radio Science*, Vol. 21, 787–796, 1986.
10. Freedman, R. and J. P. Vogiatzis, "Theory of microwave dielectric constant logging using the electromagnetic wave propagation method," *Geophysics*, Vol. 44, 969–986, 1979.
11. Wharton, R. P., R. N. Rau, and D. L. Best, "Electromagnetic propagation logging: Advances in technique and interpretation," *SPE 9267*, 1, 12, Dallas, Texas, 1980.
12. Calvert, T. J. and L. E. Wells, "Electromagnetic propagation: A new dimension in logging," *SPE 6542*, 32–43, Bakersfield, California, 1977.
13. Song, Y.-L., G. Chen, and M. Chang, "Study and application of electromagnetic logging in Daqing oilfield," *Petroleum Geological Development in Daqing*, Vol. 16, No. 4, 1997.
14. Schmitt, D. P., A. Al-Harbi, P. Saldungaray, R. Akkurt, and T. Zhang, "Revisiting dielectric logging in Saudi Arabia: Recent experiences and applications in development and exploration wells," *SPE/DGS*, 1–18, Al-Khobar, Saudi Arabia, 2011.
15. Freeman, D. W. and K. C. Henry, "Improved saturation determination with EPT," *SPE 11466*, Manama, Bahrain, 1983.
16. Al-Yaarubi, A., R. Al-Mjeni, J. Bildstein, K. Al-Ani, M. Mikhasev, F. Legendre, and M. Hizem, "Applications of dielectric dispersion logging in oil-based mud," *SPWLA 55th Annual Logging Symposium*, 18–22, Abu Dhabi, United Arab Emirates, 2014.
17. Berryman, J. G., "Mixture theories for rock properties," *Rock Physics and Phase Relations — A Handbook of Physical Constants*, 205–228, 1995.
18. Passey, Q. R., S. Creaney, J. B. Kulla, F. J. Moretti, and J. D. Stroud, "A practical model for organic richness from porosity and resistivity logs," *AAPG Bulletin*, Vol. 74, No. 12, 1777–1794, 1990.
19. Chew, W. C., "Modeling of the dielectric logging tool at high frequencies: Theory," *IEEE Transactions on Geoscience and Remote Sensing*, Vol. 26, No. 4, 382–387, 1988.
20. Donadille, J. M. and O. Faivre, "Water complex permittivity model for dielectric logging," *SPE 172566-MS*, Manama, Bahrain, 2015.